Peer-reviewed version available at *Int. J. Mol. Sci.* **2018**, *20*, 82; doi:10.3390/ijms20010082

Article

Shot-gun proteomic analysis on roots of Arabidopsis *pldα1* mutants suggesting new roles of PLDα1 in mitochondrial protein import, vesicular trafficking and glucosinolate biosynthesis

Tomáš Takáč[1], Olga Šamajová[1], Pavol Vadovič[1], Tibor Pechan[2], Jozef Šamaj[1]*

[1] Centre of the Region Haná for Biotechnological and Agricultural Research, Faculty of Science, Palacký University, Šlechtitelů 27, 783 71 Olomouc, Czech Republic; tomas.takac@upol.cz, olga.samajova@upol.cz, pavol.vadovic@upol.cz, jozef.samaj@upol.cz

[2] Institute for Genomics, Biocomputing & Biotechnology, Mississippi Agricultural and Forestry Experiment Station, Mississippi State University, MS 39759, USA; pechan@ra.msstate.edu

* Correspondence: jozef.samaj@upol.cz; Tel.: +420 585634978

Abstract: Phospholipase Dα1 (PLDα1) belongs to phospholipases, a large phospholipid hydrolyzing protein family. PLDα1 has a substrate preference for phosphatidylcholine leading to enzymatic production of phosphatidic acid, a lipid second messenger with multiple cellular functions. PLDα1 itself is implicated in biotic and abiotic stress responses. We present here a shot-gun differential proteomic analysis on roots of two *pldα1* mutants compared to the Col-0 wild type. Our data suggest new roles of PLDα1 in endomembrane transport, mitochondrial protein import and protein quality control and glucosinolate biosynthesis. Thus, we identified proteins involved in endocytosis, endoplasmic reticulum-Golgi transport and attachment sites of endoplasmic reticulum and plasma membrane (V-type proton ATPases, protein transport protein SEC13 homolog A, vesicle-associated protein 1-2, vacuolar protein sorting-associated protein 29, syntaxin-32, all upregulated in the mutants), mitochondrial import and electron transport chain (mitochondrial import inner membrane translocase subunits TIM23-2 and TIM13, mitochondrial NADH dehydrogenases, ATP synthases, cytochrome c oxidase subunit 6b-1, ADP,ATP carrier protein 2, downregulated in the mutants) and glucosinolate biosynthesis (3-isopropylmalate dehydrogenases 1, 2 and 3, methylthioalkylmalate synthase 1, cytochrome P450 83B1, Glutathione S-transferase F9, indole glucosinolate O-methyltransferase 1, adenylyl-sulfate kinase 1, all upregulated in mutants). Our results suggest broader biological roles of PLDα1 as anticipated so far.

Keywords: phospholipase D alpha1, Arabidopsis, proteomics, mitochondrial protein import, quality control, vesicular transport, cytoskeleton.

1. Introduction

Phospholipases are phospholipid hydrolyzing enzymes with multiple roles in biotic and abiotic stress responses of plants as well as in plant growth and development [1]. Phospholipase D (PLD) alpha 1 is a member of D subfamily of phospholipases and it shows the highest expression levels among all twelve PLD members in Arabidopsis [2]. Total PLD activity is substantially decreased in Arabidopsis *pldα1* mutant [3]. PLDs utilize preferentially phosphatidylcholine as a substrate which they hydrolyze in Ca^{2+} dependent manner [2]. This hydrolysis is accompanied with the production of phosphatidic acid (PA), a second messenger bearing important signalling functions [4]. Absence

Peer-reviewed version available at Int. J. Mol. Sci. 2018, 20, 82; doi:10.3390/ijms20010082

of PLDα1 leads to the reduction of cellular PA pool and membrane lipid remodeling [5,6].This remodeling affects physical and mechanical properties of membranes leading to endomembrane reorganizations and changes in membrane transport [7,8]. PLDα1 is also involved in the regulation of cytoskeletal dynamics and organization, which is either mediated by PA or by direct binding/association of PLDα1 with cytoskeleton [9,10,3,11,12]. PLDα1 promotes stomata closure and inhibits their opening [13]. At molecular level, stomatal movements are governed by PLDα1 through interaction of PA with protein phosphatase 2C (ABI1) [5], NADPH oxidase [14], sphingosine kinase [15], and microtubule associated protein 65-1[3]. In addition, PLDα1 binds and modulates components of G protein complex during stomatal movements [16,17]. These functions render PLDα1 as an important regulator of plant stress response, growth and development. Indeed, PLDα1 was shown to be involved in plant response to drought [18], cold [19] and salt stress [12]. This protein has promising biotechnological applications, since its genetic manipulation modulates plant response to abiotic stresses [20]. Nevertheless, PLDs usually act cooperatively (including the production of cellular PA pool), as it was previously exemplified in ABA induced stomatal closure [21]. Arabidopsis mutants of *PLDα1* exhibit conditional phenotypes, whereas under control conditions they show phenotypes similar to the wild-type plants [3,22]. Recent detailed fluorescent *in vivo* imaging of PLDα1 fused to YFP and expressed in Arabidopsis PLDα1 t-DNA insertion mutants under its own promoter showed that PLDα1-YFP localized to the cytoplasm in the close vicinity of PM and it exerted developmentally dependent and tissue specific expression [12]. Interestingly, most of PLDα1 functions are assigned to processes occurring in leaves. On the other hand, PLDα1 functions in roots are obscure. Shot gun proteomic analysis on genetically modified plants proved to be very useful tool for elucidation of protein functions. Here, we performed a comparative shot gun proteomic analysis on roots of two t-DNA insertion mutants (*pldα1-1* and *pldα1-2*) as compared to the Col-0 wild type. Our results indicate that PLDα1 is involved in mitochondrial protein import and quality control, glucosinolate biosynthesis and it controls very specific processes of subcellular vesicular transport.

2. Results

2.1. Overview of differential root proteomes in two pldα1 mutants

We carried out a comparative shot-gun proteomic analysis of roots of two *pldα1* mutants compared to the Col-0 as a wild type. Ninety one proteins with changed abundances were found in *pldα1-1*, while 113 were identified in *pldα1-2* mutant (Figure 1A). Thirty two proteins were commonly changed in both mutants (Figure 1B, Table 1). PLDα1 was identified uniquely in wild type, while we did not detect this protein in two studied mutants, confirming the reliability of our approach. Similarly, we were unable to detect PLDrp1 (PLD regulated protein 1; At5g39570), a phosphoprotein interacting with PLDα1 [23], in *pldα1* mutants. Complete list of all differentially abundant proteins (DAPs) of both mutants is available in Table S1. Detailed outputs of protein identification in all samples is presented in Supplementary material, and deposited in PRIDE (see below).

Preprints (www.preprints.org) | NOT PEER-REVIEWED | Posted: 20 November 2018 doi:10.20944/preprints201811.0485.v1

Peer-reviewed version available at Int. J. Mol. Sci. 2018, 20, 82; doi:10.3390/ijms20010082

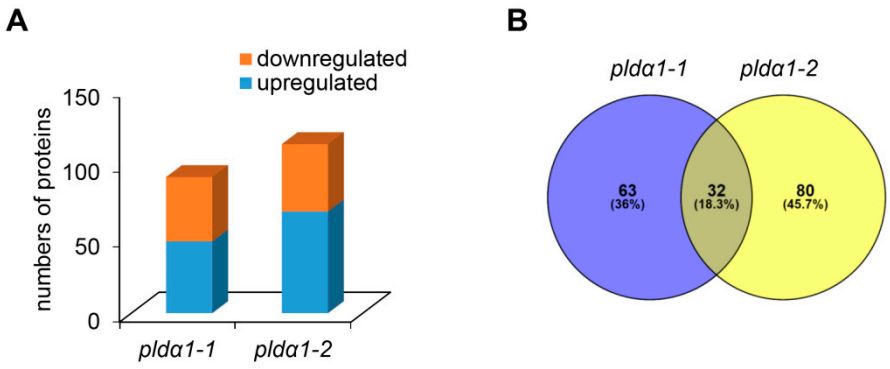

Figure 1 Overview of differential root proteomes of *pldα1* mutants. (A) Numbers of proteins with increased and decreased abundances in *pldα1-1* and *pldα1-2* mutant. (B) Venn diagram showing difference between differential proteomes the *pldα1-1* and *pldα1-2*.

Table 1 List of proteins showing significantly different abundances in roots of *pldα1-1* and *pldα1-2* mutants as compared to the wild type (Col-0).

TAIR accession number	UNIPROT accession number	Sequence Name	*pldα1-1*/ Col-0 ratio	*pldα1-2*/ Col-0 ratio	*pldα1-1*/Col-0 p value	*pldα1-2*/Col-0 p value
		Translation				
Q8LD46	At2g39460	60S ribosomal protein L23a-1	20.82	7.62	0.01	0.012
Q9LHG9	At3g12390	Nascent polypeptide-associated complex subunit alpha-like protein 1	1.82	1.91	0.052	0.029
Q9FJH6	At5g60790	ABC transporter F family member 1	Unique in WT	0.38	n.a.	0.03
		Stress response				
P50700	At4g11650	Osmotin-like protein OSM34	0.42	0.26	0.048	0.039
Q9LYW9	At5g03160	DnaJ protein P58IPK homolog	4.03	4.11	0.004	0.026
P24102	At2g38380	Peroxidase 22	1.79	1.99	0.031	0.005
Q9LSY7	At3g21770	Peroxidase 30	Unique in mutant	Unique in mutant	n.a.	n.a.
P42760	At1g02930	Glutathione S-transferase F6	0.29	0.26	0.049	0.029
Q9SRY5	At1g02920	Glutathione S-transferase F7	0.31	0.25	0.053	0.036
Q38882	At3g15730	Phospholipase D alpha 1	Unique in WT	Unique in WT	n.a.	n.a.
Q9FKA5	At5g39570	Uncharacterized protein At5g39570 (PLD regulated protein1, PLDRP1)	Unique in WT	Unique in WT	n.a.	n.a.
P32961	At3g44310	Nitrilase 1	1.79	1.79	0.018	0.023
		Membrane transport				
Q9SRI1	At3g01340	Protein transport protein SEC13 homolog A	2.55	2.97	0.001	0.011
Q8S9J8	At4g32285	Probable clathrin assembly protein At4g32285	Unique in WT	Unique in WT	n.a.	n.a.
		Mitochondrial respiratory chain				
Q9FT52	At3g52300	ATP synthase subunit d, mitochondrial	1.69	1.57	0.047	0.046
O81845	At3g54110	Mitochondrial uncoupling protein 1	1.67	2.14	0.02	0.01
P93306	AtMg00510	NADH dehydrogenase [ubiquinone] iron-sulfur protein 2	0.50	0.56	0.028	0.054
Q9S7L9	At1g22450	Cytochrome c oxidase subunit 6b-1	Unique in mutant	Unique in mutant	n.a.	n.a.

		Glucosinolate biosynthesis				
O49340	At2g30750	Cytochrome P450 71A12	Unique in WT	Unique in WT	n.a.	n.a.
Q9FG67	At5g23010	Methylthioalkylmalate synthase 1, chloroplastic	1.13	1.74	0.01	0.036
		Other functions				
Q9LSB4	At3g15950	TSA1-like protein	1.33	1.71	0.049	0.003
Q9SP02	At5g58710	Peptidyl-prolyl cis-trans isomerase CYP20-1	1.13	1.56	0.004	0.013
Q8VYV7	At5g66120	3-dehydroquinate synthase, chloroplastic	0.39	0.44	0.046	0.01
Q9AV97	At1g79500	2-dehydro-3-deoxyphosphooctonate aldolase 1	Unique in mutant	Unique in mutant	n.a.	n.a.
Q9FHR8	At5g43280	Delta(3,5)-Delta(2,4)-dienoyl-CoA isomerase, peroxisomal	0.44	0.30	0.011	0.003
Q9FIK7	At5g47720	Probable acetyl-CoA acetyltransferase, cytosolic 2	0.59	1.71	0.042	0.055
Q9FLQ4	At5g55070	Dihydrolipoyllysine-residue succinyltransferase component of 2-oxoglutarate dehydrogenase complex 1, mitochondrial	8.28	5.54	0.008	0.029
Q9FMT1	At5g14200	3-isopropylmalate dehydrogenase 3, chloroplastic	1.49	1.61	0.002	0.01
Q9LQ04	At1g63000	Bifunctional dTDP-4-dehydrorhamnose 3,5-epimerase/dTDP-4-dehydrorhamnose reductase	1.38	1.60	0.038	0.029
Q9SA14	At1g31180	3-isopropylmalate dehydrogenase 1, chloroplastic	1.52	1.55	0.019	0.02
Q9SIU0	At2g13560	NAD-dependent malic enzyme 1, mitochondrial	4.99	2.10	0.011	0.009

2.2. Classification of root differential proteomes in pldα1 mutants

KEGG pathways analysis is a reasonable tool for the evaluation of proteins involved in metabolism. The highest number of DAPs was classified into the purine metabolism pathway and biosynthesis of antibiotics. Several proteins affected in both mutants are involved in pyruvate metabolism, aminoacid biosynthesis and metabolism, and phenylpropanoid biosynthesis (Figure 2).

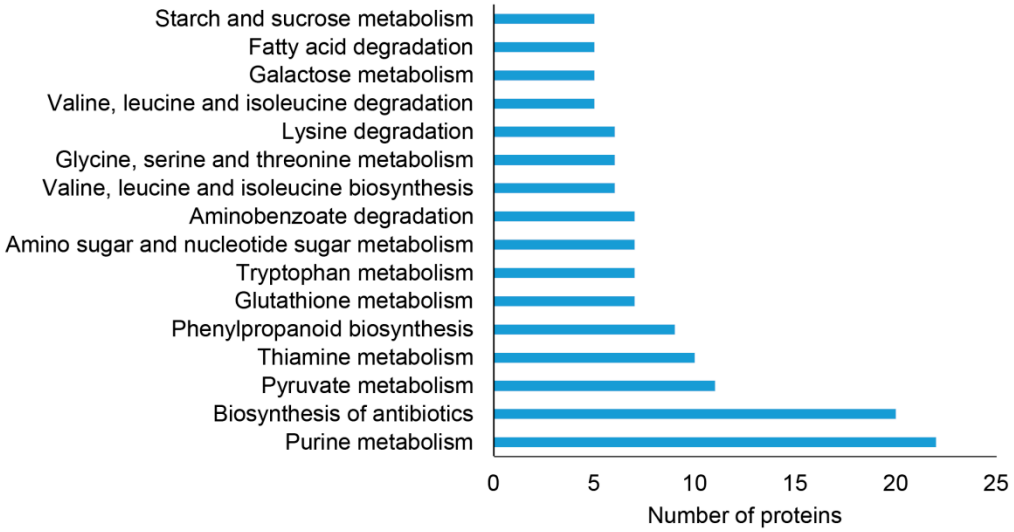

Figure 2 Functional classification of differentially abundant proteins found in roots of *pldα1-1* and *pldα1-2* mutants using KEGG pathways analysis.

We also screened differential proteomes of both mutants for the abundance of protein families, as evaluated by the Blast2Go software using InterPro application (Figure 3, Table S2). We identified 9 proteins belonging to NAD(P) binding protein superfamily, while 7 proteins belonged to Winged helix DNA-binding domain superfamily. Later ones include proteins with different functions (Table S2) and possess specific DNA binding mechanisms different from sequence specific binding. They

Peer-reviewed version available at Int. J. Mol. Sci. 2018, 20, 82; doi:10.3390/ijms20010082

display an exposed patch of hydrophobic residues implicated in protein-protein interactions [24]. Peroxidases and aldolase-type TIM barrel protein family represent abundant protein classes found in both *pldα1* mutants (Figure 3, Table S2). These proteins might show higher sensitivity to PLDα1 and PA deregulation in Arabidopsis.

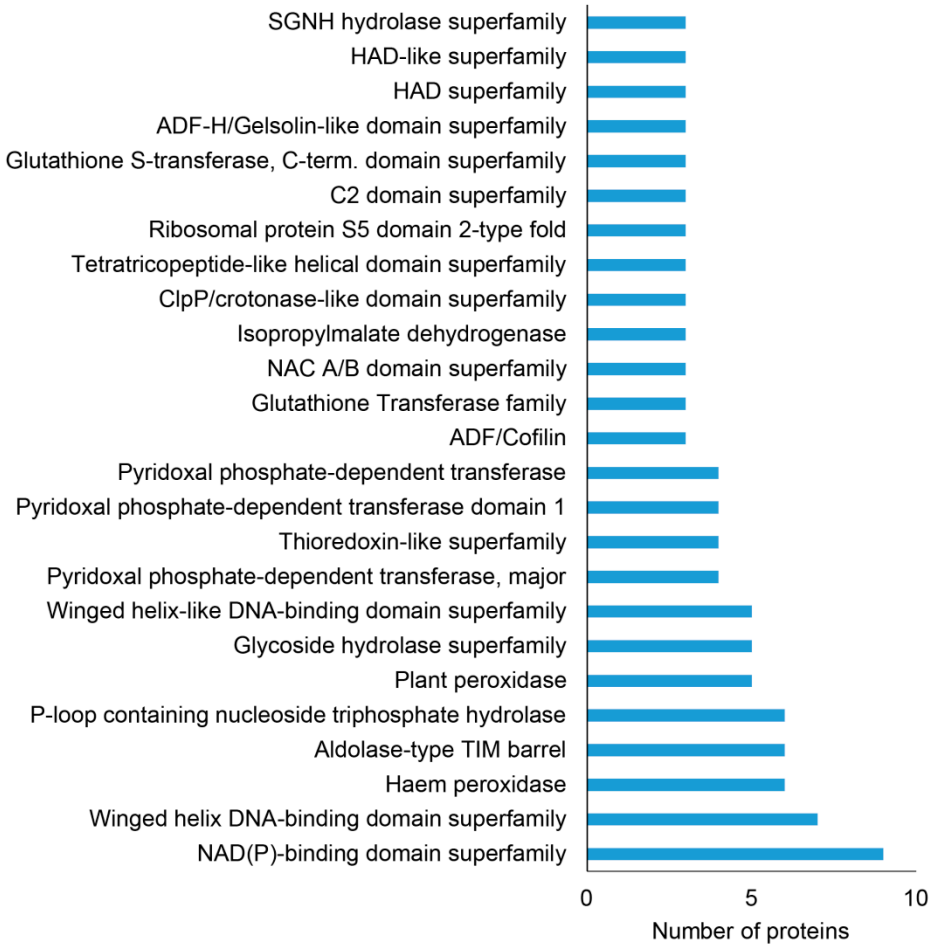

Figure 3 Distribution of protein families, in differential proteomes of *pldα1* mutants, as evaluated by InterPro application of Blast2Go software.

Further, we classified differential proteomes of *pldα1* mutants (combined) using GO annotation analysis. The highest number of the DAPs was assigned to metabolic processes and nitrogen compound metabolic processes. Significant number of DAPs was involved in response to stress as well as establishment of localization (Figure 4A). Higher levels of GO revealed that proteins annotated as involved in stress response belong to GO class called response to osmotic stress (Table S3). In addition, we also detected deregulation of proteins involved in drought, oxidative and biotic stress response (Table 1 and S1). Notably, PLDα1 deficiency in both mutants negatively affected the abundance of protein C2-domain ABA-related 10 (CAR10), a component of PYR/PYL/CAR receptors for abscisic acid (ABA) [25]. We also noticed the significant disturbance of antioxidant defense and redox homeostasis. This is represented by increased abundance of FeSOD1, ascorbate peroxidase and peptide methionine sulfoxide reductase B6. Secretory peroxidases exhibited varying changes in protein abundance, while catalase and glutathione S-transferase F7 had lower abundance in the mutants compared to wild type. To prove the increased abundance of FeSOD1, we performed an immunoblotting analysis on *pldα1* mutants using anti-FeSOD1 polyclonal primary antibody (Figure 5A, B). *Arabidopsis thaliana* genome contains 3 isoforms of FeSOD, out of which FeSOD2 and FeSOD3 are not expressed in the roots. Therefore, anti-FeSOD antibody recognizes FeSOD1 in the Arabidopsis roots. These analyses showed significant upregulation of FeSOD1 abundance in both *pldα1* mutants.

Peer-reviewed version available at Int. J. Mol. Sci. 2018, 20, 82; doi:10.3390/ijms20010082

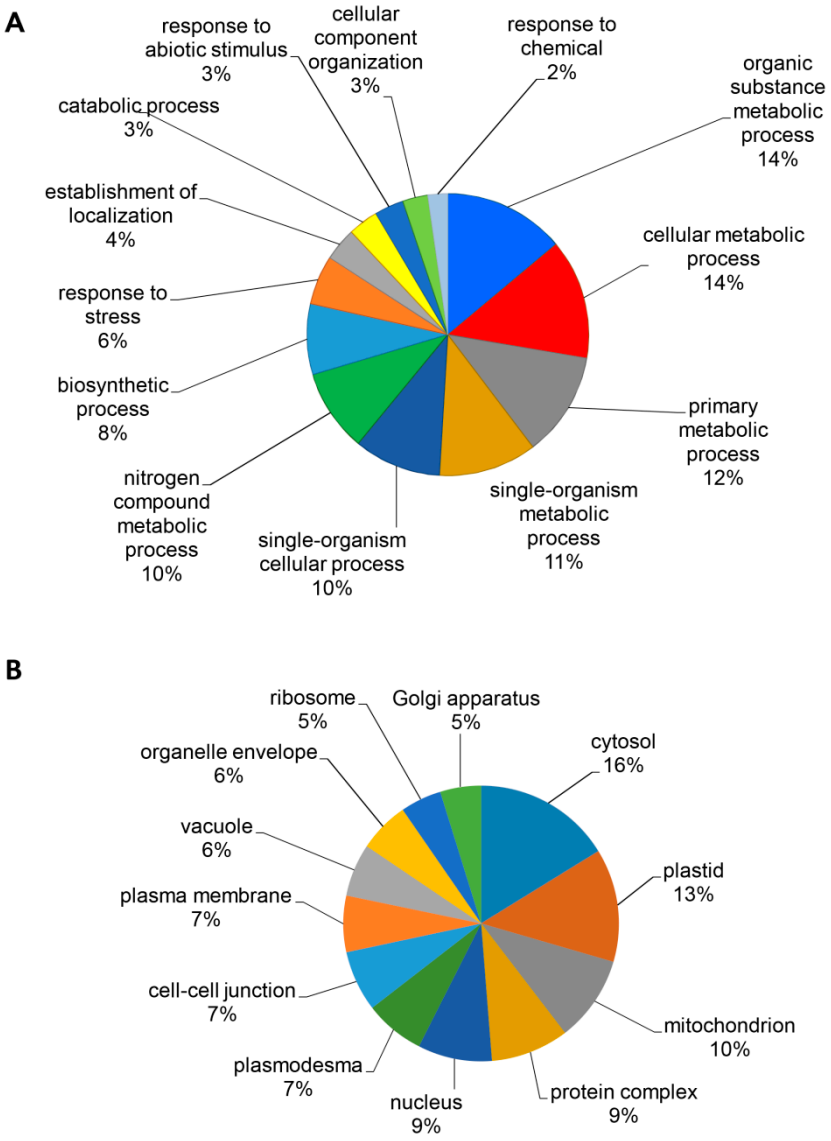

Figure 4 Functional classification of differentially abundant proteins found in roots of *pldα1-1* and *pldα1-2* mutants using Gene onthology annotation according to biological process (A; third level of onthology) and compartment (B).

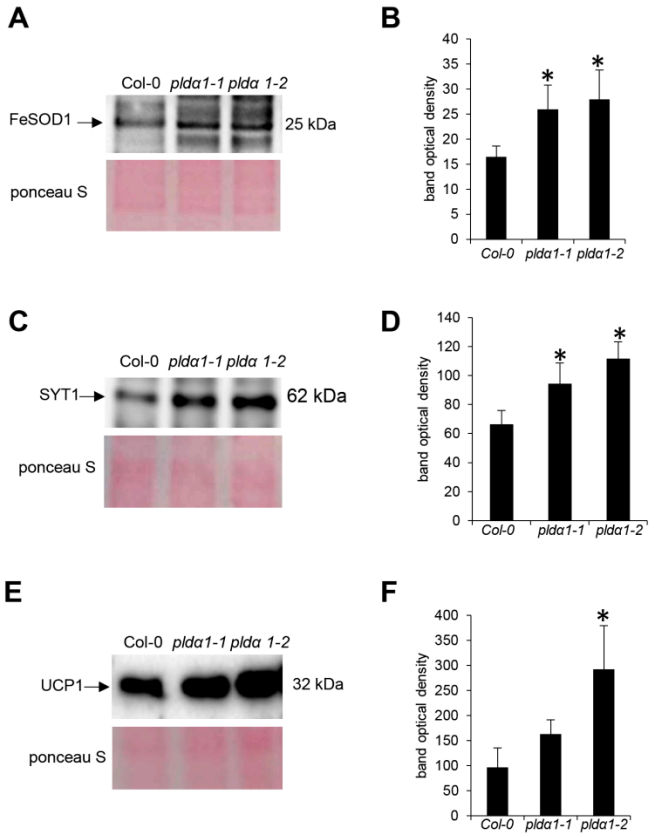

Figure 5 Immunoblotting analysis of ironic superoxide dismutase 1 (FeSOD1), syntaptotagmin 1 (SYT1) and mitochondrial uncoupling protein 1 (UCP1) in roots of Arabidopsis wild type and *pldα1* mutants. (A, C, E) Immunoblots probed with anti-FeSOD (A), anti-SYT1 (B) and anti-UCP1 (C) antibodies and visualization of proteins transferred on nitrocellulose membranes using Ponceau S. (B, D, F) Optical density quantification of respective bands in (A, C and E). Stars indicate significant differences between mutants and wild type at $p \leq 0.05$ according to the Student t-test. Error bars represent standard deviations.

Proteins classified as involved in establishment of localization account for proteins connected to transport (Table S3). This GO annotation gathers proteins involved in transport of molecules or compartments within or between cells (http://amigo.geneontology.org/amigo/term/GO:0006810). In agreement, the GO annotation analysis performed in terms of localization revealed significant numbers of proteins localized to plasmodesmata and Golgi apparatus (Figure 4B).

We have found numerous proteins involved in membrane fusion and transport. They are in detail described in Discussion. Among others, PLDα1 deficiency resulted in accumulation of synaptotagmin 1 in the mutants. These proteomic data were successfully validated using immunoblotting analyses (Figure 5C, D) and immunolocalization of SYT1 protein in intact roots showing an increased accumulation in both *pldα1* mutants (Figure 6).

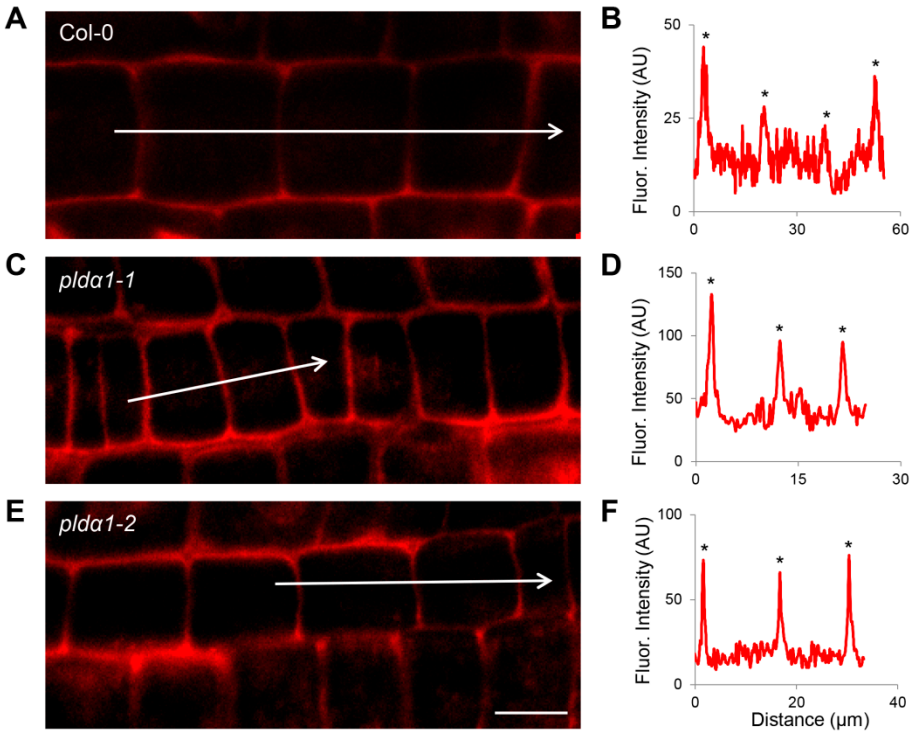

Figure 6 Immunolocalization of synaptotagmin (SYP1) in root epidermal cells of wild type (A), *pldα1-1* (C) and *pldα1-2* (E). (B, D, F) Fluorescence intensity profiles of immunolabeled synaptotagmin distributions in wild type (B), *pldα1-1* (D) and *pldα1-2* (F). Arrows indicate positions of measured cells for fluorescence intensity profiles. Asterisks indicate peaks of highest fluorescence intensities in measured cells. Note that fluorescence intensities in *pldα1* mutants are much higher in comparison to the wild type, indicating overabundance of SYP1 in these mutants. Scale bar = 10μm

In order to evaluate protein-protein interactions and protein co-expression affected in *pldα1* mutants, we subjected differential proteomes to STRING analysis (Figure 7). We have found nine protein clusters with various numbers of proteins.

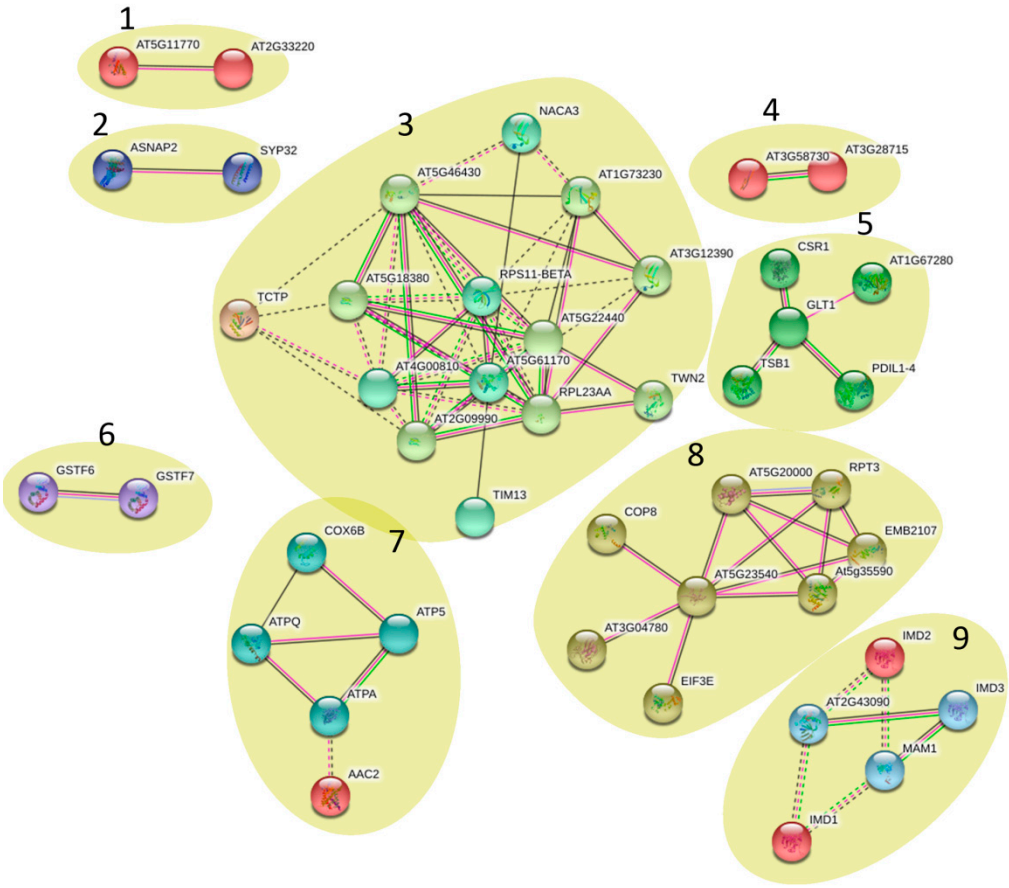

158

159 Figure 7 Depiction of protein interaction networks in combined differential proteome of both *pldα1* mutants as
160 constructed using STRING web based application. Co-expressions and protein-protein interactions based on
161 experimental evidence are considered. Note that co-expressions and interactions of homologous and
162 heterologous proteins are also taken into account. The diagram was prepared using medium confidence.
163 Cluster 1 includes At2g33220 (NADH dehydrogenase [ubiquinone] 1 alpha subcomplex subunit 13-B and
164 Atg11770 (NADH dehydrogenase [ubiquinone] iron-sulfur protein 7 mitochondrial). Cluster 2 includes SYP32
165 (Syntaxin-32) and ASNAP2 (Alpha-soluble NSF attachment protein 2). Cluster 3 includes TWN2 (Valine-tRNA
166 ligase, mitochondrial 1), TIM13 (Mitochondrial import inner membrane translocase subunit TIM13), At1g73230
167 (Nascent polypeptide-associated complex subunit beta), At2g09990 (40S ribosomal protein S16-1), RPL23AA
168 (60S ribosomal protein L23a-1), At3g12390 (Nascent polypeptide-associated complex subunit alpha-like
169 protein 1), TCTP (Translationally-controlled tumor protein 1), At4g00810 (60S acidic ribosomal protein P1-2),
170 NACA3 (Nascent polypeptide-associated complex subunit alpha-like protein 3), At5g18380 (40S ribosomal
171 protein S16-3), At5g22440 (60S ribosomal protein L10a-3), RPS11-BETA (40S ribosomal protein S11-3),
172 At5g46430 60S ribosomal protein L32-2), At5g61170 (40S ribosomal protein S19-3). Cluster 4 includes
173 At3g28715 (V-type proton ATPase subunit d2) and At3g58730 (V-type proton ATPase subunit D). Cluster 5
174 includes At1g67280 (Probable lactoylglutathione lyase, chloroplastic), CSR1 (Acetolactate synthase,
175 chloroplastic), GLT1 (Glutamate synthase 1 [NADH], chloroplastic), TSB1 (Tryptophan synthase beta chain 1,
176 chloroplastic) and PDIL1-4 (Protein disulfide isomerase-like 1-4). Cluster 6 includes GSTF7 (Glutathione
177 S-transferase F7 and GSTF6, Cluster 7 includes COX6B (Cytochrome c oxidase subunit 6b-1), ATPQ (ATP
178 synthase subunit d, mitochondrial), ATP5 (ATP synthase subunit O, mitochondrial), AAC2 (ADP,ATP carrier
179 protein 2, mitochondrial) and ATPA (ATP synthase subunit alpha, chloroplastic). Cluster 8 includes At3g04780
180 (PITH domain-containing protein At3g04780), EIF3E (Eukaryotic translation initiation factor 3 subunit E),
181 EMB2107 (26S proteasome non-ATPase regulatory subunit 12 homolog A), At5g20000 (26S proteasome
182 regulatory subunit 8 homolog B), At5g23540 (26S proteasome non-ATPase regulatory subunit 14 homolog),
183 At5g35590 (Proteasome subunit alpha type-6-A), COP8 (COP9 signalosome complex subunit 4) and RPT3 (26S
184 proteasome regulatory subunit 6B homolog). Cluster 9 includes IMD3 (3-isopropylmalate dehydrogenase 1,
185 chloroplastic), IMD2 (3-isopropylmalate dehydrogenase 2, chloroplastic), IMD1 (3-isopropylmalate

Peer-reviewed version available at Int. J. Mol. Sci. 2018, 20, 82; doi:10.3390/ijms20010082

dehydrogenase 3, chloroplastic), MAM1 (Methylthioalkylmalate synthase 1, chloroplastic) and At2g43090 (3-isopropylmalate dehydratase small subunit 3).

The most abundant cluster is represented by proteins involved in ribosome biogenesis, which are co-expressed with mitochondrial valine-tRNA ligase (important nucleus encoded component of the mitochondrial protein synthesis), mitochondrial import inner membrane translocase subunit TIM13 (component of the mitochondrial protein import machinery) and subunits of nascent polypeptide-associated complex. These findings might indicate defects of cytosolic translation and mitochondrial protein import resulting in changed abundances of mitochondrial proteins. Therefore we searched for proteins carrying mitochondrial targeting signal among DAPs. We have found 19 proteins with varying changes in their abundance, suggesting an altered homeostasis in the import of mitochondrial proteins (Table S4). One of such proteins, mitochondrial uncoupling protein 1 (UPC1) has increased abundance in the mutants, being in agreement with the immunoblotting analysis (Figure 5E, F) and immunolocalization of UCP1 protein (Figure 8). In addition, we observed also decreased levels of MORF8 (multiple site organellar RNA editing factor, designated also as RIP1; Table S1), a protein important for mitochondrial mRNA editing. Finally, absence of PLDα1 in both mutants affects also a cluster of components of the mitochondrial respiratory chain. Thus, PLDα1 is likely required for multiple mitochondrial functions in Arabidopsis.

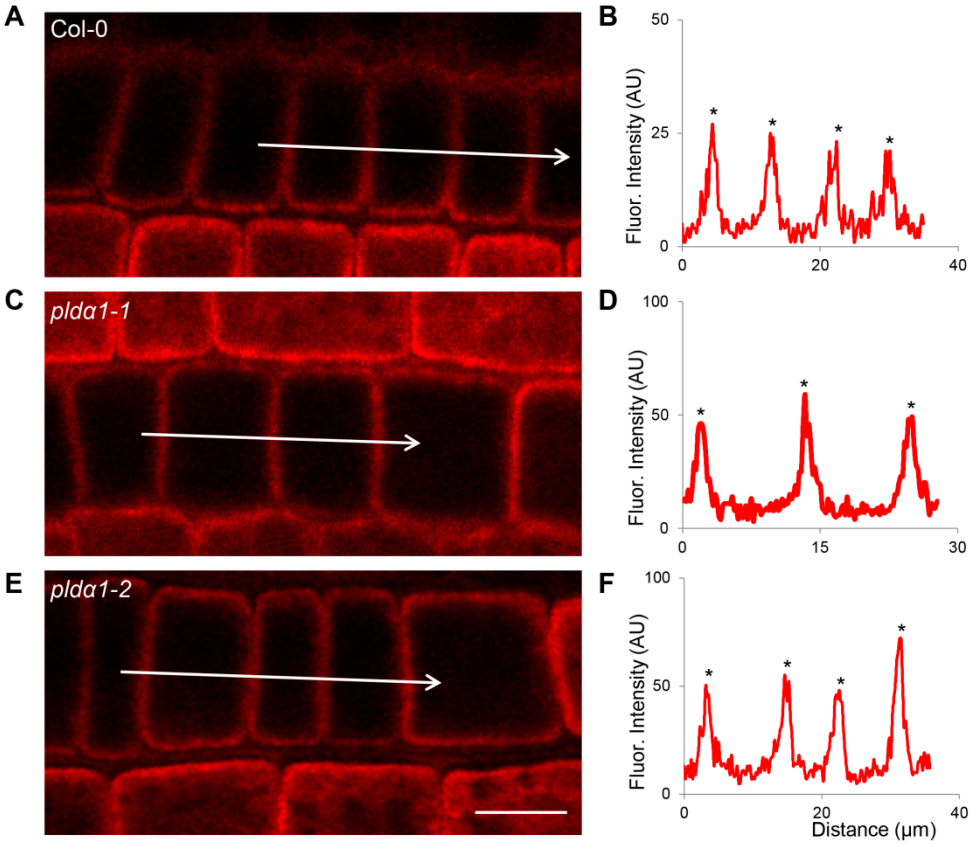

Figure 8 Immunolocalization of mitochondrial uncoupling protein 1 (UCP1) in root epidermal cells of wild type (A), *pldα1-1* (C) and *pldα1-2* (E). (B, D, F) Fluorescence intensity profiles of immunolabeled synaptotagmin distributions in wild type (B), *pldα1-1* (D) and *pldα1-2* (F). Arrows indicate positions of measured cells for fluorescence intensity profiles. Asterisks indicate peaks of highest fluorescence intensities in measured cells. Note that fluorescence intensities in *pldα1* mutants are much higher in comparison to the wild type, indicating overabundance of UCP1 in these mutants. Scale bar = 10μm

Other protein cluster is mostly composed by proteins belonging to proteasome complex, which are co-expressed with PITH domain-containing protein At3g04780 (protein with unknown function), eukaryotic translation initiation factor 3 subunit E (translation regulator) and COP8

(subunit of the COP9 signalosome).We also identified protein clusters composed of proteins involved in glucosinolate and aminoacid biosynthesis (Figure 7).

PLDα1 and PA are important regulators of actin and microtubule cytoskeletons in plants [11,26]. As expected, PLDα1 deficiency in both mutants resulted also in differential abundances of actin and microtubule associated proteins, including actin1 and actin depolymerizing factors (ADFs) 1, 8 and 10 (showing decreased abundances in *pldα1* mutants) (Table 1 and S1). Such results indicate possible disturbances in actin monomer turnover and actin polymerization in *pldα1* mutants. We also identified two protein candidates potentially important for microtubule regulation by PLDα1. Both proteins were detected uniquely in *pldα1* mutants and are involved in tubulin monomer folding. Tubulin-folding cofactor B, is a member of the Arabidopsis PILZ group proteins [27,28]. It interacts with alpha-tubulin and its overexpression results in reduced number of microtubules [29]. Chaperone prefoldin 6 is required for tubulin monomer abundance, microtubule dynamics and organization [30].

3. Discussion

This differential proteomic analysis on roots of *pldα1* mutants revealed that PLDα1 is required for homeostasis of proteins involved in diverse processes. In this study, we focused especially on potential new functions of PLDα1 such as mitochondrial protein import and quality control, vesicular trafficking and glucosinolate biosynthesis. Considering the regulatory and catalytic roles of PLDα1, we assume that besides its lipid hydrolyzing activity, the changes in the proteomes of *pldα1* mutants occurred as a consequence of compromised PA, G protein complex and ABA signalling.

3.2. Mitochondrial protein import and quality control

According to our results, PLDα1 deficiency in mutants caused a deregulation of proteins involved in protein import to mitochondria, including mitochondrial import inner membrane translocase subunits TIM23-2 and TIM13, which are downregulated. While TIM23-2 is a translocase responsible for the transport of mitochondrial precursor proteins carrying a cleavable N-terminal pre-sequence [31], TIM13 is a member of small TIM complex delivering client precursors that pass through the TOM channel to Tim22 in the mitochondrial intermembrane space [32]. Therefore, the import of nucleus-encoded mitochondrial proteins is altered in *pldα1* mutants. Along with altered protein import to mitochondria, PLDα1 deficiency may affect also N-terminal presequence cleavage (inferred by increased abundance of presequence protease 1 in *pldα1* mutants) occurring after protein precursor import into mitochondria [33]. Furthermore, we provide experimental evidence on deregulation of prohibitin 6 involved in mitochondrial protein folding [34]. Prohibitins (PHBs) are considered as structural proteins that form a scaffold-like structure for interacting with a set of proteins involved in various mitochondrial processes [34]. These proteins participate in the assembly of multi-subunit complexes such as mitochondrial respiratory complex [35]. Accordingly, several proteins of the mitochondrial electron transport chain show significant changes in their abundance in both mutants as compared to the wild type. Mitochondrial protein import machinery was also reported to be in close interaction with the organization of respiratory complexes. Tim23-2 is localized also in respiratory complex 1 and its genetic modification leads to altered transcription of mitochondrial proteins and defective mitochondria biogenesis [31]. Similar role in mitochondria biogenesis was found also for prohibitins [36]. So far, PLDα1 was not linked to these mitochondrial functions, although ATP synthase subunit gamma and ADP/ATP carrier protein were targeted by PA in Arabidopsis [37].

3.2. Vesicular transport

PLD derived PA can regulate membrane transport by direct modification of membrane curvature or by recruiting important regulatory proteins [38]. These proteins positively affect protein internalization [39,40], vesicle fusion and aggregation [41]. In Drosophila, PLD activity

Peer-reviewed version available at Int. J. Mol. Sci. 2018, 20, 82; doi:10.3390/ijms20010082

couples endocytosis with retromer dependent recycling [42]. Our findings indicate that PLDα1 alters multiple sites of endomembrane system. For example, in both mutants we detected decreased abundances of vacuolar H^+ ATPases (subunits D and d2), which control multiple events in endomembrane transport by acidification of endomembrane compartments [43].

In accordance with the known involvement of PLDs in vesicle fusions, we observed an increased abundance of alpha-soluble NSF attachment protein 2 (Alpha-SNAP2) in the *pldα1-1* mutant. Alpha-SNAP proteins bind the SNARE complex [44] and are required for the vesicle pre-docking, an initial step of the membrane fusion reaction [45,46]. The precise function of alpha-SNAP2 is unknown so far, but it might require PLDα1. Remarkably, alpha-SNAP2 interacting SYP32, a Golgi localized Qa SNARE [47] was found as upregulated in *pldα1* mutants. Thus, PLDα1 might be necessary for SNARE-SNAP protein complexes stability.

We identified several proteins involved in the endocytic pathway as differentially regulated in both *pldα1* mutants. These include mainly the probable clathrin assembly protein At4g32285 (not detected in *pldα1* mutants), which is involved in clathrin-mediated endocytosis [48]. Clathrin assembly proteins interact directly with proteins of the clathrin coat and are able to bind phospholipids [49]. Two such proteins were identified as PA-binding proteins [37]. Furthermore, PLDα1 localized in the vicinity of clathrin heavy chain and microtubules of Arabidopsis root cells [12] may directly bind clathrin in a complex containing adaptor protein-2 (AP-2) [50]. VPS29, a protein found uniquely in the *pldα1-1* mutant, is a component of retromer complex. This is a coat complex localized to the cytosolic face of endosomes and involved in intracellular sorting of some transmembrane proteins [51]. VPS29 is important for normal morphology of prevacuolar compartment (PVC) and plays crucial role in recycling vacuolar sorting receptors from the PVC to the *trans* Golgi network (TGN) during trafficking of soluble proteins to the lytic vacuole [52,53]. These data uncovers new endocytic proteins affected in *pldα1* mutants.

PLDα1 deficiency in both mutants altered also abundances of proteins involved in the regulation of ER to Golgi transport. Protein transport protein SEC13 homolog A is almost threefold upregulated in both *pldα1* mutants. Sec13 makes a lattice structure together with Sec31 to form COPII vesicles [54], which are responsible for ER to Golgi transport. According to our results, PLDα1 may have also an impact on the morphology of Golgi apparatus, inferred by upregulation of Golgin candidate 5 (also known as TATA element modulatory factor) in the *pldα1-2* mutant [55,56]. Another protein important for ER to Golgi trafficking is vesicle-associated protein 1-2 (PVA12, also known as VAP27-3), which is upregulated in the *pldα1-1* mutant. This is an ER-localized protein belonging to a VAP27 family [57]. It binds to oxysterol-binding protein-related protein 3B [58], which is also upregulated in the mutants and is proposed to cycle between the ER and the Golgi [58]. Recently, PVA12 was shown to colocalize and interact with Networked 3C (NET3C) at ER–plasma membrane (PM) contact sites [57]. Considering PLDα1 localization in the plasma membrane (PM) vicinity, we may suggest an involvement of this protein in ER-PM attachment. This is emphasized also by increased abundance of synaptotagmin 1 (SYT1) in *pldα1* mutants, representing a protein mediating the ER-PM contacts in Arabidopsis [59].

PLDα1 depletion leads to changed abundance of proteins regulating the membrane transport. Changes in protein level might be a result of deregulation of protein synthesis and proteolysis or transcriptional control. Previously it was shown that changes in membrane transport might result in changed abundance of proteins. This was exemplified for example in Arabidopsis roots exposed to brefeldin A which blocks secretion/exocytosis by aggregation of TGN and PM-derived vesicles surrounded by Golgi stacks into so called BFA-compartments [60]. Altered endocytosis and vacuolar trafficking by wortmannin lead to altered abundances of vacuolar proteases potentially leading to defected protein degradation [61]. Similar downregulation of such protease, subtilisin-like protease SBT1.7 is encountered also in roots of *pldα1* mutants. Based on our proteomic data we suggest that this dynamics of membrane transport regulatory processes might result from defected protein degradation and as a feedback mechanism of PLDα1 depletion-induced changes in membrane architecture, membrane transport and PA accumulation.

3.3. Glucosinolate biosynthesis

PLDs have been shown to crosstalk with hormonal signalling in plants. In addition to their well-known role in ABA signalling, they also participate in salicylic acid signalling by controlling relocation of NPR1, an essential regulator of SA induced gene transcription, into nucleus [62]. In addition, PLDs might be activated by cytokinins [63] and ethylene (Fan et al., 1997). CTR1, a negative regulator of ethylene response is a potential target of PA [64]. PLDs are also involved in auxin distribution. Thus, PLDζ-derived PA is required for PP2AC recruitment to the membrane resulting in altered PIN1 phosphorylation and polar distribution [7]. Auxins share an initial steps of biosynthetic pathway with glucosinolates [65,66]. Arabidopsis mutants with reduced glucosinolate contents show severe auxin phenotypes [67]. Generally, glucosinolates are secondary messengers produced in *Brassicaceae* with important defense and developmental functions [65,68]. PLDα1 deficiency in mutants causes increased abundances of enzymes involved in glucosinolate biosynthesis, including four subunits of 3-isopropylmalate dehydrogenase and methylthioalkylmalate synthase, all involved in the chain elongation machinery. Enzymes involved in the biosynthesis of the core glucosinolate structure, namely cytochrome P450 83B1, glutathione S-transferase F9, indole glucosinolate O-methyltransferase 1 and adenylyl-sulfate kinase 1 show similar trends in their abundances (Table S1). PLDa1 induced an imbalance of indole glucosinolate o-methyltransferase 1 abundance, which is a glucosinolate modifying enzyme [66]. Glutathione synthase 1 shows increased abundance in mutants, most likely contributing to the glutathione pool, which serves as a sulfur donor within the second stage of GLS biosynthesis [66]. Such differential regulation of enzymes involved in one metabolic pathway in untargeted proteomic approach is very unusual, suggesting that PLDα1 might be a master regulator of glucosinolate biosynthesis. It is likely, that this regulation is mediated via PA, since cytochrome P450 83B1 is a PA-binding protein, as identified in a proteomic screen [37]

4. Materials and Methods

4.1. Plant material

Seeds of *Arabidopsis thaliana* wild type (ecotype Col-0) as well as *pldα1-1* (SALK_067533) and *pldα1-2* (SALK_053785) t-DNA insertion mutants were used in this study. Following ethanol surface-sterilization, they were cultivated vertically on solid half-strength MS media at 21°C under 16/8 light/dark illumination conditions for 14 days. Roots were quickly dissected and harvested for protein extraction. Proteomic analyses were performed in 4 biological replicates. Roots of 30 seedlings were pooled in one biological replicate.

4.2. Protein extraction and trypsin digestion

Samples were ground in liquid nitrogen and subjected to phenol protein extraction followed by ammonium acetate/methanol precipitation as described by Takáč et al. [69]. Cleaned precipitates were dissolved in 6 M urea in 100 mM Tris (pH 7,8). Prior to trypsin digestion, extracts containing 50 µg of proteins (in volume of 50 µl) were diluted with 100 mM Tris-HCl (pH7,8) to adjust the urea concentration bellow 1 mM. Proteins were digested with trypsin (Promega;1µg of trypsin to 50 µg of proteins) at 37 °C overnight. Reaction was stopped by addition of 4µl of acetic acid. Peptide mixtures were cleaned using C18 gravity flow cartridges (Bond Elut C18; Agilent Technologies, Santa Clara, CA) according to manufacturer's instructions. Peptides eluted by 95% acetonitrile were dried using vacuum concentrator and stored under -80°C until analysis.

4.3. Liquid chromatography, mass spectrometry, protein identification and relative quantitative analysis

LC-MSMS and protein identification was performed as published previously [69]. Briefly, two micrograms of protein tryptic digest were loaded on reversed phase Acclaim PepMap C18 column (Thermo Fisher Scientific, Waltham, MA, USA). A constant flow (0.3 µl.min^{-1}), 170-minute long

nonlinear gradient of acetonitrile in 0.1% formic acid (2%-55% for 125 min, 95% for 15 min, 2% for 30 min) was used to separate and elute peptides. The mass spectra were collected in the data dependent acquisition mode in 18 scan events: one MS scan (m/z range: 300–1700) followed by 17 MSMS scans for the 17 most intense ions detected in MS scan (with dynamic exclusion being applied). The method and raw spectral files were created and generated, respectively, by Xcalibur 2.1 (Thermo Fisher Scientific). The files were analyzed using the SEQUEST algorithm of the Proteome Discoverer 1.1.0 software (Thermo Fisher Scientific). Variable modifications were set as follows: cysteine carbamidomethylation (+57.021), methionine oxidation (+15.995), methionine dioxidation (+31.990). The spectral data were matched against target and decoy databases for more stringent approach to estimate false discovery rates (FDR), compared to single search of concatenated database. The UNIPROT (www.uniprot.org) Arabidopsis genus taxonomy Reviewed protein database (17,586 entries as of September 2017) served as the target database, while its reversed copy (created automatically by the software) served as a decoy database. The search results were filtered by FDR < 1%. Identified proteins were grouped by default parameters of the software, defining the group as proteins strictly necessary to explain presence of identified peptides. A representative/master protein of the group is the protein with highest score, spectral count and number of matched peptides. If these parameters are equal, the protein with longest sequence is designated as a master protein. Proteins listed in the supplementary materials are master proteins. If the peptide can be attributed to more than one protein, it is indicated by multiple protein accession numbers allocated to the given peptide. This is also shown in supplementary .xls files. The mass spectrometry proteomics data have been deposited to the ProteomeXchange Consortium via the PRIDE partner repository with the dataset identifier PXD011196.

The relative quantitative analysis was done using the ProteoIQ 2.1 (NuSep) software as published previously [70]. It was based on sums of precursor ion intensities (PII) of filtered peptides attributed to given proteins. Summed intensities pertinent to proteins in individual replicates were normalized by factors that were calculated to equalize total intensity of all master proteins across all biological samples and replicates. Normalized average protein intensities were used to calculate fold changes when comparing biological samples. All data points were considered. The ANOVA $p \leq 0.05$ was used to filter statistically significant results. Proteins with fold change higher than 1.5 were considered as differentially abundant.

4.4 Bioinformatic analysis

Gene ontology (GO) annotation analysis of differentially abundant proteins (DAPs) was performed using Blast2Go software [71]. Blast searching was performed against *Arabidopsis thaliana* NCBI database allowing 1 BLAST Hit. The annotation was carried out by using these parameters: E Value Hit filter: $1.0E^{-6}$; Annotation cut off: 55; GO weight: 5. STRING [72] database was used for analysis of protein interaction network among DAPs applying minimum required interaction score 0.7, relevant for high confidence prediction. The prediction of presence of mitochondrial targeting pre-sequence in differential proteomes of both mutants was performed using MitoFates [73].

4.5. Immunoblotting analysis

Roots of fourteen days old plants were homogenized using liquid nitrogen in mortar with pestle. The proteins were extracted in 50mM Hepes (pH 7.5) containing 75 mM NaCl, 1 mM EGTA, 1 mM $MgCl_2$, 10% (v/v) glycerol, 1 mM DTT and Complete® EDTA free protease inhibitor cocktail (Roche). Following 15 min incubation on ice and subsequent centrifugation at 13000 g for 15 min, the extracts were desalted using Amicon Ultra centrifugal filters (with 10 kDa cutoff) according to the manufacturer instructions. Proteins were quantified using the Bradford assay and the extracts were supplemented with 4 times concentrated SDS sample buffer to reach final concentration of 62.5 mM Tris-HCl, pH 6.8, 2% (w/v) SDS, 10% (v/v) glycerol and 300 mM 2-mercaptoethanol. Following 5min boiling at 95°C, equal amount of proteins were loaded on 12% or 17% Stain free gels (BioRad) and the electrophoresis run at constant 150V at RT. Proteins were transferred to nitrocellulose membranes using TransBlot Turbo blotting apparatus (BioRad) and the proteins were visualized on

membranes using Ponceau S. Membranes were incubated overnight in 4% BSA/4% nonfat milk in Tris-buffered saline containing 1% Tween-20 at 4°C. Following blocking, membranes were incubated overnight at 4°C in TBST supplemented with 1% BSA and primary antibodies in following dilutions: anti-synaptotagmin antibody (PhytoAb; 1:1000); anti-FeSOD (Agrisera; 1:3000); anti-UCP1 (Agrisera; 1:1000). Afterwards, the membranes were washed repeatedly in TBST and incubated in HRP-conjugated secondary antibody (F(ab')2-goat anti-rabbit IgG (H+L) Secondary Antibody, HRP; Thermo Fisher Scientific) diluted to 1:5000 in 1% (w/v) BSA in TBST. The signal was developed using Clarity™ ECL Western Blotting Substrate (BioRad) and documented on ChemiDoc™ documentation system (BioRad). Band densities were quantified using ImageLab software (BioRad). All immunoblot analyses were performed at least in 3 biological replicates. Student's t-test was applied to evaluate the statistical significance of differences.

4.6. Whole mount immunofluorescence labelling

Immunolocalization of SYP1 and UCP1 proteins in root wholemounts was done as described previously [74]. Samples were immunolabeled with rabbit anti-synaptotagmin 1 antibody (PhytoAb; 1:200) and anti-UCP1 antibody (Agrisera; 1:200) in 3% (w/v) BSA in PBS at 4°C overnight. Secondary Alexa-Fluor 647 goat anti-rabbit IgGs antibodies were diluted 1:500 in PBS containing 3% (w/v) BSA for 3 h (1.5 h at 37 °C and 1.5 h at room temperature). Immunolabeled samples were analysed with a Zeiss 710 Confocal Laser Scanning Microscope (CLSM) platform (Carl Zeiss, Jena, Germany), using excitation lines at 405 and 561 nm from argon, HeNe, diode and diode pumped solid-state lasers. Fluorescence intensity was evaluated using ZEN 2010 software (Carl Zeiss). Images were processed using ZEN 2010 software, Photoshop 6.0/CS, and Microsoft PowerPoint.

Supplementary Materials: Supplementary materials can be found online.

Author Contributions: J.Š. conceived and coordinated the experiments and helped to evaluate data, T.T., T.P., O.Š., P.V. made analyses and experiments, T.T. and J.Š. wrote the manuscript. All authors reviewed the manuscript.

Funding: This research was supported by Grant No. 16-22044S from the Czech Science Foundation GACR, USDA NIFA award # 58-6066-6-059 and NIH award # USM-GR05802-03.

Acknowledgments: The mass spectrometry proteomics analysis was performed at the Institute for Genomics, Biocomputing and Biotechnology, Mississippi State University, with partial support from Mississippi Agriculture and Forestry Experimental Station.

Conflicts of Interest: The authors declare no conflict of interest. The funders had no role in the design of the study; in the collection, analyses, or interpretation of data; in the writing of the manuscript, or in the decision to publish the results.

References

1. *Phospholipases in Plant Signaling*; Wang, X., Ed.; Signaling and Communication in Plants; Springer Berlin Heidelberg: Berlin, Heidelberg, 2014; Vol. 20; ISBN 978-3-642-42010-8.
2. Hong, Y.; Zhao, J.; Guo, L.; Kim, S.-C.; Deng, X.; Wang, G.; Zhang, G.; Li, M.; Wang, X. Plant phospholipases D and C and their diverse functions in stress responses. *Prog. Lipid Res.* **2016**, *62*, 55–74, doi:10.1016/j.plipres.2016.01.002.
3. Zhang, Q.; Lin, F.; Mao, T.; Nie, J.; Yan, M.; Yuan, M.; Zhang, W. Phosphatidic acid regulates microtubule organization by interacting with MAP65-1 in response to salt stress in Arabidopsis. *Plant Cell* **2012**, *24*, 4555–4576, doi:10.1105/tpc.112.104182.

4. Testerink, C.; Munnik, T. Molecular, cellular, and physiological responses to phosphatidic acid formation in plants. *J. Exp. Bot.* **2011**, *62*, 2349–2361, doi:10.1093/jxb/err079.
5. Zhang, W.; Qin, C.; Zhao, J.; Wang, X. Phospholipase D alpha 1-derived phosphatidic acid interacts with ABI1 phosphatase 2C and regulates abscisic acid signaling. *Proc. Natl. Acad. Sci. U. S. A.* **2004**, *101*, 9508–9513, doi:10.1073/pnas.0402112101.
6. Devaiah, S.P.; Roth, M.R.; Baughman, E.; Li, M.; Tamura, P.; Jeannotte, R.; Welti, R.; Wang, X. Quantitative profiling of polar glycerolipid species from organs of wild-type Arabidopsis and a PHOSPHOLIPASE Dα1 knockout mutant. *Phytochemistry* **2006**, *67*, 1907–1924, doi:10.1016/j.phytochem.2006.06.005.
7. Gao, H.-B.; Chu, Y.-J.; Xue, H.-W. Phosphatidic Acid (PA) Binds PP2AA1 to Regulate PP2A Activity and PIN1 Polar Localization. *Mol. Plant* **2013**, *6*, 1692–1702, doi:10.1093/mp/sst076.
8. Boutté, Y.; Moreau, P. Modulation of endomembranes morphodynamics in the secretory/retrograde pathways depends on lipid diversity. *Curr. Opin. Plant Biol.* **2014**, *22*, 22–29, doi:10.1016/j.pbi.2014.08.004.
9. Dhonukshe, P.; Laxalt, A.M.; Goedhart, J.; Gadella, T.W.J.; Munnik, T. Phospholipase d activation correlates with microtubule reorganization in living plant cells. *Plant Cell* **2003**, *15*, 2666–2679, doi:10.1105/tpc.014977.
10. Pleskot, R.; Potocký, M.; Pejchar, P.; Linek, J.; Bezvoda, R.; Martinec, J.; Valentová, O.; Novotná, Z.; Zárský, V. Mutual regulation of plant phospholipase D and the actin cytoskeleton. *Plant J.* **2010**, *62*, 494–507, doi:10.1111/j.1365-313X.2010.04168.x.
11. Pleskot, R.; Li, J.; Žárský, V.; Potocký, M.; Staiger, C.J. Regulation of cytoskeletal dynamics by phospholipase D and phosphatidic acid. *Trends Plant Sci.* **2013**, *18*, 496–504, doi:10.1016/j.tplants.2013.04.005.
12. Novák, D.; Vadovič, P.; Ovečka, M.; Šamajová, O.; Komis, G.; Colcombet, J.; Šamaj, J. Gene Expression Pattern and Protein Localization of Arabidopsis Phospholipase D Alpha 1 Revealed by Advanced Light-Sheet and Super-Resolution Microscopy. *Front. Plant Sci.* **2018**, *9*, 371, doi:10.3389/fpls.2018.00371.
13. Mishra, G.; Zhang, W.; Deng, F.; Zhao, J.; Wang, X. A bifurcating pathway directs abscisic acid effects on stomatal closure and opening in Arabidopsis. *Science* **2006**, *312*, 264–266, doi:10.1126/science.1123769.
14. Zhang, Y.; Zhu, H.; Zhang, Q.; Li, M.; Yan, M.; Wang, R.; Wang, L.; Welti, R.; Zhang, W.; Wang, X. Phospholipase Dα1 and Phosphatidic Acid Regulate NADPH Oxidase Activity and Production of Reactive Oxygen Species in ABA-Mediated Stomatal Closure in Arabidopsis. *Plant Cell* **2009**, *21*, 2357–2377, doi:10.1105/tpc.108.062992.
15. Guo, L.; Mishra, G.; Markham, J.E.; Li, M.; Tawfall, A.; Welti, R.; Wang, X. Connections between sphingosine kinase and phospholipase D in the abscisic acid signaling pathway in Arabidopsis. *J. Biol. Chem.* **2012**, *287*, 8286–8296, doi:10.1074/jbc.M111.274274.
16. Roy Choudhury, S.; Pandey, S. The role of PLDα1 in providing specificity to signal-response coupling by heterotrimeric G-protein components in Arabidopsis. *Plant J.* **2016**, *86*, 50–61, doi:10.1111/tpj.13151.

17. Roy Choudhury, S.; Pandey, S. Phosphatidic acid binding inhibits RGS1 activity to affect specific signaling pathways in Arabidopsis. *Plant J.* **2017**, *90*, 466–477, doi:10.1111/tpj.13503.
18. Hong, Y.; Zheng, S.; Wang, X. Dual functions of phospholipase Dalpha1 in plant response to drought. *Mol. Plant* **2008**, *1*, 262–269, doi:10.1093/mp/ssm025.
19. Huo, C.; Zhang, B.; Wang, H.; Wang, F.; Liu, M.; Gao, Y.; Zhang, W.; Deng, Z.; Sun, D.; Tang, W. Comparative Study of Early Cold-Regulated Proteins by Two-Dimensional Difference Gel Electrophoresis Reveals a Key Role for Phospholipase Dα1 in Mediating Cold Acclimation Signaling Pathway in Rice. *Mol. Cell. Proteomics* **2016**, *15*, 1397–1411, doi:10.1074/mcp.M115.049759.
20. Lu, S.; Bahn, S.C.; Qu, G.; Qin, H.; Hong, Y.; Xu, Q.; Zhou, Y.; Hong, Y.; Wang, X. Increased expression of phospholipase Dα1 in guard cells decreases water loss with improved seed production under drought in Brassica napus. *Plant Biotechnol. J.* **2013**, *11*, 380–389, doi:10.1111/pbi.12028.
21. Uraji, M.; Katagiri, T.; Okuma, E.; Ye, W.; Hossain, M.A.; Masuda, C.; Miura, A.; Nakamura, Y.; Mori, I.C.; Shinozaki, K.; et al. Cooperative function of PLDδ and PLDα1 in abscisic acid-induced stomatal closure in Arabidopsis. *Plant Physiol.* **2012**, *159*, 450–460, doi:10.1104/pp.112.195578.
22. Devaiah, S.P.; Pan, X.; Hong, Y.; Roth, M.; Welti, R.; Wang, X. Enhancing seed quality and viability by suppressing phospholipase D in Arabidopsis: Phospholipase D in seed aging. *Plant J.* **2007**, *50*, 950–957, doi:10.1111/j.1365-313X.2007.03103.x.
23. Ufer, G.; Gertzmann, A.; Gasulla, F.; Röhrig, H.; Bartels, D. Identification and characterization of the phosphatidic acid-binding *A. thaliana* phosphoprotein PLDrp1 that is regulated by PLDα1 in a stress-dependent manner. *Plant J.* **2017**, *92*, 276–290, doi:10.1111/tpj.13651.
24. Gajiwala, K.S.; Burley, S.K. Winged helix proteins. *Curr. Opin. Struct. Biol.* **2000**, *10*, 110–116.
25. Rodriguez, L.; Gonzalez-Guzman, M.; Diaz, M.; Rodrigues, A.; Izquierdo-Garcia, A.C.; Peirats-Llobet, M.; Fernandez, M.A.; Antoni, R.; Fernandez, D.; Marquez, J.A.; et al. C2-domain abscisic acid-related proteins mediate the interaction of PYR/PYL/RCAR abscisic acid receptors with the plasma membrane and regulate abscisic acid sensitivity in Arabidopsis. *Plant Cell* **2014**, *26*, 4802–4820, doi:10.1105/tpc.114.129973.
26. Pleskot, R.; Pejchar, P.; Staiger, C.J.; Potocký, M. When fat is not bad: the regulation of actin dynamics by phospholipid signaling molecules. *Front. Plant Sci.* **2014**, *5*, doi:10.3389/fpls.2014.00005.
27. Steinborn, K. The Arabidopsis PILZ group genes encode tubulin-folding cofactor orthologs required for cell division but not cell growth. *Genes Dev.* **2002**, *16*, 959–971, doi:10.1101/gad.221702.
28. Du, Y.; Cui, M.; Qian, D.; Zhu, L.; Wei, C.; Yuan, M.; Zhang, Z.; Li, Y. AtTFC B is involved in control of cell division. *Front. Biosci. Elite Ed.* **2010**, *2*, 752–763.

29. Dhonukshe, P.; Bargmann, B.O.R.; Gadella, T.W.J. Arabidopsis Tubulin Folding Cofactor B Interacts with α-Tubulin In Vivo. *Plant Cell Physiol.* **2006**, *47*, 1406–1411, doi:10.1093/pcp/pcl001.
30. Gu, Y.; Deng, Z.; Paredez, A.R.; DeBolt, S.; Wang, Z.-Y.; Somerville, C. Prefoldin 6 is required for normal microtubule dynamics and organization in Arabidopsis. *Proc. Natl. Acad. Sci. U. S. A.* **2008**, *105*, 18064–18069, doi:10.1073/pnas.0808652105.
31. Wang, Y.; Carrie, C.; Giraud, E.; Elhafez, D.; Narsai, R.; Duncan, O.; Whelan, J.; Murcha, M.W. Dual location of the mitochondrial preprotein transporters B14.7 and Tim23-2 in complex I and the TIM17:23 complex in Arabidopsis links mitochondrial activity and biogenesis. *Plant Cell* **2012**, *24*, 2675–2695, doi:10.1105/tpc.112.098731.
32. Neupert, W. A Perspective on Transport of Proteins into Mitochondria: A Myriad of Open Questions. *J. Mol. Biol.* **2015**, *427*, 1135–1158, doi:10.1016/j.jmb.2015.02.001.
33. Teixeira, P.F.; Glaser, E. Processing peptidases in mitochondria and chloroplasts. *Biochim. Biophys. Acta BBA - Mol. Cell Res.* **2013**, *1833*, 360–370, doi:10.1016/j.bbamcr.2012.03.012.
34. Van Aken, O.; Whelan, J.; Van Breusegem, F. Prohibitins: mitochondrial partners in development and stress response. *Trends Plant Sci.* **2010**, *15*, 275–282, doi:10.1016/j.tplants.2010.02.002.
35. Piechota, J.; Bereza, M.; Sokołowska, A.; Suszyński, K.; Lech, K.; Jańska, H. Unraveling the functions of type II-prohibitins in Arabidopsis mitochondria. *Plant Mol. Biol.* **2015**, *88*, 249–267, doi:10.1007/s11103-015-0320-3.
36. Ahn, C.S.; Lee, J.H.; Reum Hwang, A.; Kim, W.T.; Pai, H.-S. Prohibitin is involved in mitochondrial biogenesis in plants. *Plant J.* **2006**, *46*, 658–667, doi:10.1111/j.1365-313X.2006.02726.x.
37. McLoughlin, F.; Arisz, S.A.; Dekker, H.L.; Kramer, G.; de Koster, C.G.; Haring, M.A.; Munnik, T.; Testerink, C. Identification of novel candidate phosphatidic acid-binding proteins involved in the salt-stress response of *Arabidopsis thaliana* roots. *Biochem. J.* **2013**, *450*, 573–581, doi:10.1042/BJ20121639.
38. Donaldson, J.G. Phospholipase D in endocytosis and endosomal recycling pathways. *Biochim. Biophys. Acta* **2009**, *1791*, 845–849, doi:10.1016/j.bbalip.2009.05.011.
39. Antonescu, C.N.; Danuser, G.; Schmid, S.L. Phosphatidic Acid Plays a Regulatory Role in Clathrin-mediated Endocytosis. *Mol. Biol. Cell* **2010**, *21*, 2944–2952, doi:10.1091/mbc.E10-05-0421.
40. Li, G.; Xue, H.-W. Arabidopsis PLD 2 Regulates Vesicle Trafficking and Is Required for Auxin Response. *Plant Cell* **2007**, *19*, 281–295, doi:10.1105/tpc.106.041426.
41. Roth, M.G. Molecular mechanisms of PLD function in membrane traffic. *Traffic Cph. Den.* **2008**, *9*, 1233–1239, doi:10.1111/j.1600-0854.2008.00742.x.
42. Thakur, R.; Panda, A.; Coessens, E.; Raj, N.; Yadav, S.; Balakrishnan, S.; Zhang, Q.; Georgiev, P.; Basak, B.; Pasricha, R.; et al. Phospholipase D activity couples plasma membrane endocytosis with retromer dependent recycling. *eLife* **2016**, *5*, doi:10.7554/eLife.18515.
43. Schumacher, K.; Krebs, M. The V-ATPase: small cargo, large effects. *Curr. Opin. Plant Biol.* **2010**, *13*, 724–730, doi:10.1016/j.pbi.2010.07.003.

44. Fujiwara, M.; Uemura, T.; Ebine, K.; Nishimori, Y.; Ueda, T.; Nakano, A.; Sato, M.H.; Fukao, Y. Interactomics of Qa-SNARE in Arabidopsis thaliana. *Plant Cell Physiol.* **2014**, *55*, 781–789, doi:10.1093/pcp/pcu038.
45. Mayer, A.; Wickner, W.; Haas, A. Sec18p (NSF)-Driven Release of Sec17p (α-SNAP) Can Precede Docking and Fusion of Yeast Vacuoles. *Cell* **1996**, *85*, 83–94, doi:10.1016/S0092-8674(00)81084-3.
46. Wang, T.; Li, L.; Hong, W. SNARE proteins in membrane trafficking. *Traffic Cph. Den.* **2017**, *18*, 767–775, doi:10.1111/tra.12524.
47. Uemura, T.; Ueda, T.; Ohniwa, R.L.; Nakano, A.; Takeyasu, K.; Sato, M.H. Systematic analysis of SNARE molecules in Arabidopsis: dissection of the post-Golgi network in plant cells. *Cell Struct. Funct.* **2004**, *29*, 49–65.
48. Wang, C.; Yan, X.; Chen, Q.; Jiang, N.; Fu, W.; Ma, B.; Liu, J.; Li, C.; Bednarek, S.Y.; Pan, J. Clathrin Light Chains Regulate Clathrin-Mediated Trafficking, Auxin Signaling, and Development in Arabidopsis. *Plant Cell* **2013**, *25*, 499–516, doi:10.1105/tpc.112.108373.
49. Fan, L.; Li, R.; Pan, J.; Ding, Z.; Lin, J. Endocytosis and its regulation in plants. *Trends Plant Sci.* **2015**, *20*, 388–397, doi:10.1016/j.tplants.2015.03.014.
50. Yamaoka, S.; Shimono, Y.; Shirakawa, M.; Fukao, Y.; Kawase, T.; Hatsugai, N.; Tamura, K.; Shimada, T.; Hara-Nishimura, I. Identification and dynamics of Arabidopsis adaptor protein-2 complex and its involvement in floral organ development. *Plant Cell* **2013**, *25*, 2958–2969, doi:10.1105/tpc.113.114082.
51. Zelazny, E.; Santambrogio, M.; Pourcher, M.; Chambrier, P.; Berne-Dedieu, A.; Fobis-Loisy, I.; Miège, C.; Jaillais, Y.; Gaude, T. Mechanisms Governing the Endosomal Membrane Recruitment of the Core Retromer in *Arabidopsis*. *J. Biol. Chem.* **2013**, *288*, 8815–8825, doi:10.1074/jbc.M112.440503.
52. Kang, H.; Kim, S.Y.; Song, K.; Sohn, E.J.; Lee, Y.; Lee, D.W.; Hara-Nishimura, I.; Hwang, I. Trafficking of Vacuolar Proteins: The Crucial Role of Arabidopsis Vacuolar Protein Sorting 29 in Recycling Vacuolar Sorting Receptor. *Plant Cell* **2012**, *24*, 5058–5073, doi:10.1105/tpc.112.103481.
53. Nodzyński, T.; Feraru, M.I.; Hirsch, S.; De Rycke, R.; Niculaes, C.; Boerjan, W.; Van Leene, J.; De Jaeger, G.; Vanneste, S.; Friml, J. Retromer Subunits VPS35A and VPS29 Mediate Prevacuolar Compartment (PVC) Function in Arabidopsis. *Mol. Plant* **2013**, *6*, 1849–1862, doi:10.1093/mp/sst044.
54. Hino, T.; Tanaka, Y.; Kawamukai, M.; Nishimura, K.; Mano, S.; Nakagawa, T. Two Sec13p Homologs, AtSec13A and AtSec13B, Redundantly Contribute to the Formation of COPII Transport Vesicles in *Arabidopsis thaliana*. *Biosci. Biotechnol. Biochem.* **2011**, *75*, 1848–1852, doi:10.1271/bbb.110331.
55. Fridmann-Sirkis, Y.; Siniossoglou, S.; Pelham, H.R.B. TMF is a golgin that binds Rab6 and influences Golgi morphology. *BMC Cell Biol.* **2004**, *5*, 18, doi:10.1186/1471-2121-5-18.
56. Latijnhouwers, M.; Gillespie, T.; Boevink, P.; Kriechbaumer, V.; Hawes, C.; Carvalho, C.M. Localization and domain characterization of Arabidopsis golgin candidates. *J. Exp. Bot.* **2007**, *58*, 4373–4386, doi:10.1093/jxb/erm304.

57. Wang, P.; Richardson, C.; Hawkins, T.J.; Sparkes, I.; Hawes, C.; Hussey, P.J. Plant VAP27 proteins: domain characterization, intracellular localization and role in plant development. *New Phytol.* **2016**, *210*, 1311–1326, doi:10.1111/nph.13857.
58. Saravanan, R.S.; Slabaugh, E.; Singh, V.R.; Lapidus, L.J.; Haas, T.; Brandizzi, F. The targeting of the oxysterol-binding protein ORP3a to the endoplasmic reticulum relies on the plant VAP33 homolog PVA12. *Plant J. Cell Mol. Biol.* **2009**, *58*, 817–830, doi:10.1111/j.1365-313X.2009.03815.x.
59. Siao, W.; Wang, P.; Voigt, B.; Hussey, P.J.; Baluska, F. Arabidopsis SYT1 maintains stability of cortical endoplasmic reticulum networks and VAP27-1-enriched endoplasmic reticulum–plasma membrane contact sites. *J. Exp. Bot.* **2016**, *67*, 6161–6171, doi:10.1093/jxb/erw381.
60. Takáč, T.; Pechan, T.; Richter, H.; Müller, J.; Eck, C.; Böhm, N.; Obert, B.; Ren, H.; Niehaus, K.; Šamaj, J. Proteomics on brefeldin A-treated Arabidopsis roots reveals profilin 2 as a new protein involved in the cross-talk between vesicular trafficking and the actin cytoskeleton. *J. Proteome Res.* **2011**, *10*, 488–501, doi:10.1021/pr100690f.
61. Takáč, T.; Pechan, T.; Šamajová, O.; Ovečka, M.; Richter, H.; Eck, C.; Niehaus, K.; Šamaj, J. Wortmannin Treatment Induces Changes in Arabidopsis Root Proteome and Post-Golgi Compartments. *J. Proteome Res.* **2012**, *11*, 3127–3142, doi:10.1021/pr201111n.
62. Janda, M.; Šašek, V.; Chmelařová, H.; Andrejch, J.; Nováková, M.; Hajšlová, J.; Burketová, L.; Valentová, O. Phospholipase D affects translocation of NPR1 to the nucleus in Arabidopsis thaliana. *Front. Plant Sci.* **2015**, *6*, 59, doi:10.3389/fpls.2015.00059.
63. Kravets, V.S.; Kretinin, S.V.; Kolesnikov, Y.S.; Getman, I.A.; Romanov, G.A. Cytokinins evoke rapid activation of phospholipase D in sensitive plant tissues. *Dokl. Biochem. Biophys.* **2009**, *428*, 264–267.
64. Testerink, C.; Larsen, P.B.; van der Does, D.; van Himbergen, J.A.J.; Munnik, T. Phosphatidic acid binds to and inhibits the activity of Arabidopsis CTR1. *J. Exp. Bot.* **2007**, *58*, 3905–3914, doi:10.1093/jxb/erm243.
65. Malka, S.K.; Cheng, Y. Possible Interactions between the Biosynthetic Pathways of Indole Glucosinolate and Auxin. *Front. Plant Sci.* **2017**, *8*, doi:10.3389/fpls.2017.02131.
66. Sønderby, I.E.; Geu-Flores, F.; Halkier, B.A. Biosynthesis of glucosinolates--gene discovery and beyond. *Trends Plant Sci.* **2010**, *15*, 283–290, doi:10.1016/j.tplants.2010.02.005.
67. Skirycz, A.; Reichelt, M.; Burow, M.; Birkemeyer, C.; Rolcik, J.; Kopka, J.; Zanor, M.I.; Gershenzon, J.; Strnad, M.; Szopa, J.; et al. DOF transcription factor AtDof1.1 (OBP2) is part of a regulatory network controlling glucosinolate biosynthesis in Arabidopsis. *Plant J. Cell Mol. Biol.* **2006**, *47*, 10–24, doi:10.1111/j.1365-313X.2006.02767.x.
68. Petersen, A.; Wang, C.; Crocoll, C.; Halkier, B.A. Biotechnological approaches in glucosinolate production. *J. Integr. Plant Biol.* **2018**, doi:10.1111/jipb.12705.

668 69. Takáč, T.; Šamajová, O.; Pechan, T.; Luptovčiak, I.; Šamaj, J. Feedback Microtubule
669 Control and Microtubule-Actin Cross-talk in Arabidopsis Revealed by Integrative
670 Proteomic and Cell Biology Analysis of KATANIN 1 Mutants. *Mol. Cell. Proteomics*
671 **2017**, *16*, 1591–1609, doi:10.1074/mcp.M117.068015.
672 70. Takáč, T.; Vadovič, P.; Pechan, T.; Luptovčiak, I.; Šamajová, O.; Šamaj, J.
673 Comparative proteomic study of Arabidopsis mutants mpk4 and mpk6. *Sci. Rep.* **2016**,
674 *6*, 28306.
675 71. Conesa, A.; Götz, S. Blast2GO: A comprehensive suite for functional analysis in plant
676 genomics. *Int. J. Plant Genomics* **2008**, *2008*, 619832, doi:10.1155/2008/619832.
677 72. Szklarczyk, D.; Franceschini, A.; Wyder, S.; Forslund, K.; Heller, D.; Huerta-Cepas, J.;
678 Simonovic, M.; Roth, A.; Santos, A.; Tsafou, K.P.; et al. STRING v10: protein-protein
679 interaction networks, integrated over the tree of life. *Nucleic Acids Res.* **2015**, *43*,
680 D447-452, doi:10.1093/nar/gku1003.
681 73. Fukasawa, Y.; Tsuji, J.; Fu, S.-C.; Tomii, K.; Horton, P.; Imai, K. MitoFates: improved
682 prediction of mitochondrial targeting sequences and their cleavage sites. *Mol. Cell.*
683 *Proteomics MCP* **2015**, *14*, 1113–1126, doi:10.1074/mcp.M114.043083.
684 74. Šamajová, O.; Komis, G.; Šamaj, J. Immunofluorescent Localization of MAPKs and
685 Colocalization with Microtubules in Arabidopsis Seedling Whole-Mount Probes.
686 *Methods Mol. Biol. Clifton NJ* **2014**, *1171*, 107–115,
687 doi:10.1007/978-1-4939-0922-3_9.